



BNL-105270-2014-TECH

Booster Technical Note No. 228;BNL-105270-2014-IR

# Au<sup>32+</sup> BEAM INTENSITY LOSSES IN THE AGS BOOSTER DUE TO CHARGE EXCHANGE PROCESSES

H. M. Calvani

October 1996

Collider Accelerator Department  
**Brookhaven National Laboratory**

**U.S. Department of Energy**

USDOE Office of Science (SC)

Notice: This technical note has been authored by employees of Brookhaven Science Associates, LLC under Contract No.DE-AC02-76CH00016 with the U.S. Department of Energy. The publisher by accepting the technical note for publication acknowledges that the United States Government retains a non-exclusive, paid-up, irrevocable, world-wide license to publish or reproduce the published form of this technical note, or allow others to do so, for United States Government purposes.

## **DISCLAIMER**

This report was prepared as an account of work sponsored by an agency of the United States Government. Neither the United States Government nor any agency thereof, nor any of their employees, nor any of their contractors, subcontractors, or their employees, makes any warranty, express or implied, or assumes any legal liability or responsibility for the accuracy, completeness, or any third party's use or the results of such use of any information, apparatus, product, or process disclosed, or represents that its use would not infringe privately owned rights. Reference herein to any specific commercial product, process, or service by trade name, trademark, manufacturer, or otherwise, does not necessarily constitute or imply its endorsement, recommendation, or favoring by the United States Government or any agency thereof or its contractors or subcontractors. The views and opinions of authors expressed herein do not necessarily state or reflect those of the United States Government or any agency thereof.

**Au<sup>32+</sup> BEAM INTENSITY LOSSES IN THE AGS BOOSTER  
DUE TO CHARGE EXCHANGE PROCESSES**

**BOOSTER TECHNICAL NOTE  
NO. 228**

**H. M. Calvani and L. A. Ahrens**

**October 1, 1996**

**ALTERNATING GRADIENT SYNCHROTRON DEPARTMENT  
BROOKHAVEN NATIONAL LABORATORY  
UPTON, NEW YORK 11973**



# AU<sup>32+</sup> BEAM INTENSITY LOSSES IN THE AGS BOOSTER DUE TO CHARGE EXCHANGE PROCESSES

H. M. Calvani and L.A. Ahrens

## ABSTRACT

A study has been conducted to gain understanding of the intensity losses observed while running Au<sup>32+</sup> ions in the AGS Booster. It was determined that the intensity loss rate has a sensitive dependence on beam momentum and the injected number of Gold ions. In this work, we model the beam loss by considering two mechanisms, [i] charge exchange interactions with the residual molecular gases in the Booster vacuum chamber and [ii] intra-beam Au<sup>32+</sup> charge exchange. We present a brief review of the theory of charge exchange relevant to these processes, and compare the predictions with the measured rate coefficients and cross sections extrapolated from the data. The results for the measured beam loss vs. beam momentum are in qualitative agreement (up to a factor  $\sim 3$ ) with the losses expected due to beam-gas charge exchange interactions. On the other hand, the beam loss rate increase with beam intensity was found to be significant and any proposed mechanism for the loss has not been confirmed. In particular, the contributions of intra-beam charge exchange were quantified, and estimated to be negligible. A discussion of possible vacuum deterioration in the Booster is also presented.

## 1 INTRODUCTION

The mechanisms responsible for the beam intensity losses observed while accelerating Gold ions in the AGS Booster continue to be poorly understood. Previous studies conducted in the 1993 and 1994 heavy ion run while accelerating Au<sup>15+</sup> and Au<sup>33+</sup> suggested beam-gas interaction and degradation of the vacuum pressure as the underlying mechanism for beam loss[1,2]. In particular, for Au<sup>15+</sup>, the beam survival time was limited by the observed sensitive dependence with the injected number of ions. During the 1995 run, the scheme consisted of stripping Au<sup>12+</sup> from the Tandem accelerator to Au<sup>32+</sup> before injection into the Booster at a momentum of 41.5 MeV/c/nucleon<sup>1</sup>. This note consists of a study undertaken in order to probe the beam loss properties for Au<sup>32+</sup>. Emphasis was placed on understanding

<sup>1</sup>The Booster injection momentum is set by the Tandem voltage, and was not changed throughout the study.

the dependence of beam intensity losses with beam momentum, the number of ions in the Booster, and determining and comparing the extrapolated cross section for charge exchange interactions (electron capture and stripping) with the theoretical predictions. Also of particular interest is to model the beam loss by the inclusion of charge exchange processes (intra-beam charge exchange) between Gold ions in the beam (eg. Au<sup>32+</sup> + Au<sup>32+</sup> → Au<sup>31+</sup> + Au<sup>33+</sup>).

The contributions of ion intra-beam charge exchange have been previously considered in storage rings (eg. HIBALL II, heavy ion fusion accelerator) running scenarios with Au<sup>1-</sup> ions [3]. In such machines, the limit of acceptable storage time is affected by the large number of ions ( $N_{Au^{1-}} \sim 10^{15}$  ions), leading to a higher number of ion-ion interactions and consequently shorter beam lifetimes. In the case of the Booster, the relatively lower ion intensity ( $N \sim 10^8 - 10^9$  ions) and fast acceleration cycle would suggest intra-beam charge exchange to be of minimal effect. Indeed, experimental evidence against the importance of intra-beam charge exchange has been noted in previous Booster studies with Au<sup>15+</sup>, where the beam loss rates have been observed to remain constant independent of whether the beam is bunched or not [1]. At any rate, the corresponding probability (rate constant) for such a mechanism in the Booster has never been quantified. In this work we present the first experimental estimates of the rate constant and cross section for Au<sup>32+</sup> intra-beam interactions, thus quantifying the contribution of such a mechanism in the Booster. Studying these effects is not only an important source of information about atomic collisions and processes in complex atomic systems; but also of utmost interest as we attempt to reach the desired Gold beam intensity required for the operation of the Relativistic Heavy Ion Collider (RHIC).

## 2 VACUUM RELATED BEAM LOSSES

The charge state of heavy ion beams in the AGS Booster can change due to interactions with the residual molecular gases present in the vacuum chamber. The dominant mechanisms responsible for these interactions are

electron capture and loss (stripping)<sup>2</sup>. These processes have a sensitive energy dependence, and occur with high probabilities. Any such change in charge leads to immediate beam loss from the Booster due to the incompatibility between the magnetic rigidity set in the machine lattice, and that required for the newly formed heavy ion charge state. Discussion of these processes in the Booster have been previously studied by Hseuh[4] with Au<sup>33+</sup> among other heavy ion species. In the following we briefly recapitulate the relevant formulae describing beam-gas charge exchange.

## 2.1 ELECTRON CAPTURE

To predict the cross section for single electron capture by the heavy ions, we employ the empirical scaling rule proposed by A.S. Schlachter et al. [5], which gives the best agreement (fit) to pre-existing experimental data, and allows for a determination of cross sections for a variety of projectile-gas target systems. It is expressed in terms of generalized reduced coordinates by

$$\tilde{\sigma} = \sigma_c Z_T^{1.8} / Q^{0.5}, \quad \tilde{E} = E / (Z_T^{1.25} Q^{0.7}), \quad (1)$$

where  $\sigma_c$  is the electron capture cross section,  $Q$  the ion charge state,  $E$  the ion energy (MeV) per nucleon and  $Z_T$  the atomic number of the gas target. The capture cross section  $\sigma_c$  [cm<sup>2</sup>] is then determined through  $\tilde{\sigma}$  by the expression

$$\tilde{\sigma} = \frac{1.1 \times 10^{-8}}{\tilde{E}^{4.8}} \left[ 1 - \exp\left(-0.037 \tilde{E}^{2.2}\right) \right] \times \left[ 1 - \exp\left(-2.44 \times 10^{-5} \tilde{E}^{2.6}\right) \right]. \quad (2)$$

Eq. (2) above, is valid for reduced energies in the range  $10 < \tilde{E} < 1000$ , and applicable to the heavy ion energies involved in this study. It is important to note that the contributions of electron capture to beam loss are predominant at low ionic energies and decrease rapidly as the beam energy increases.

## 2.2 ELECTRON LOSS (STRIPPING)

The loss of one or more electrons from the heavy ions results from ionization processes, whereby energy transfer to the electrons by interactions with the residual gas particles is sufficient to overcome the ionization potential of the atomic nuclear field. To describe the process, a modified empirical version of the Bohr Linhard formulae developed by Betz [6] is used:

$$\sigma_s \sim 9.0 \times 10^{-19} Q^{-3} Z_T Z_P \beta^{-1} [\text{cm}^2]. \quad (3)$$

<sup>2</sup>Nuclear and multiple Coulomb scattering are expected to be several orders of magnitude smaller. Their contributions are therefore neglected.

Here,  $Z_P$  corresponds to the atomic number of the heavy ion (projectile),  $\beta$  the relativistic parameter ( $v/c$ ), and  $Q$  and  $Z_T$  as described in eq.(1). Note the strong dependence of the stripping cross section on the ion charge state ( $\sigma_s(\text{Au}^{15+}) \sim 10\sigma_s(\text{Au}^{32+})$ ). In contrast with electron capture processes, the electron loss cross section decreases in magnitude very slowly with increasing  $\beta$ , and its effects are dominant at higher energies.

## 2.3 MODELING CHARGE EXCHANGE BEAM-GAS LOSSES

To first approximation, the rate of beam loss in the Booster can be parametrized by the first order differential equation

$$\frac{dN}{dt} = -\alpha N(t), \quad (4)$$

where  $N(t)$  represents the number of ions in the Booster as a function of time, and  $\alpha$  the average beam loss rate. To describe charge exchange interactions with the residual molecular gases in the vacuum chamber, we expect the loss rate  $\alpha$  to be a function of the total charge exchange cross section ( $\sigma_t = \sigma_c + \sigma_s$ ), the interacting ion velocity ( $\beta c$ ), and the number density of molecules in the vacuum chamber. We can derive such a relation from simple kinetic principles. Given that the interaction mean free path between the heavy ions and residual gas molecules reads

$$l = \beta c \tau = (n \sigma_t)^{-1}, \quad (5)$$

where  $c$  is the speed of light,  $\tau$  the mean free time between successive interactions,  $n$  the number density of gas particles, and  $\sigma_t$  the total charge exchange cross section calculated from eq's (1) and (3), we can approximate the loss rate (inverse beam-lifetime after integration through the cycle) as

$$\alpha \sim \frac{1}{\tau} = \sigma_t n \beta c. \quad (6)$$

It readily follows from integration of eq.(4) after substitution of eq.(6), and imposing the initial boundary condition  $N(t=0) = N_0$ , that we can express the fraction of beam loss after transversing a distance  $dl = \beta c dt$  as

$$\frac{N}{N_0} = \exp\left(-\int_0^l \sigma_t n dl\right). \quad (7)$$

Where  $N_0$  denotes the initial number of ions in the Booster.

## 2.4 MEASUREMENTS OF BEAM-GAS LOSSES

In order to study the dependence of beam-gas losses with beam momentum, the length of the Booster main magnet cycle was increased from the 200 ms used for Heavy Ion Physics program to 800 ms, and was configured to include intervals of constant magnetic field. The magnitude of the magnetic plateau was varied accordingly, and the momentum of the Gold ions was confirmed from revolution frequency measurements taken using a frequency analyzer. The data consisted of normalized current transformer traces taken at the end of the acceleration cycle when the RF system was turned off non-adiabatically, and the debunched beam was allowed to coast for the remaining time of the cycle ( $\sim 600 - 700$ ms). In addition, before the beam loss data was recorded, the machine was tuned, and transfer and acceleration efficiencies were optimized.

The vacuum conditions in the Booster were specified by quadrupole mass spectrometer measurements, which yielded a residual gas species distribution of 43 %  $H_2$ , 27%  $CH_4$ , 23%  $CO_2$  and 7%  $CO$  [7]<sup>3</sup>. The measured ring average pressure corresponded to  $5.6 \times 10^{-11}$ Torr, which, at an average temperature  $\bar{T} = 250$  K, the ideal gas law equation of state yields a uniform number density of  $2.1 \times 10^6$  molecules/cm<sup>3</sup>.

Figures 1-5 display the data taken for the different beam momenta ( $\beta$ 's) at comparable intensities ( $4.6 \sim \times 10^8$ ions @ RF turn off) with a 730 us pulse width. A median filter has been used to remove unphysical high frequency structure from the current transformer traces while maintaining edge information. The solid line represents a least squares fit to the data, and the dashed lines the theoretical capture and strip loss rates, and their combined contribution predicted by eq (7)(refer to legend). For purposes of comparison, note that the calculated loss rates has been constrained to graphically intersect the measured best line fit. The results, as presented in Table I, include the predicted and measured total charge exchange cross sections and the corresponding average loss rates.

Some interesting results emerged from Table I. First, the rate of beam loss decreases substantially and progressively as the beam momenta is increased. Inspection of Figures 1 and 5 indicates that for  $\beta = 0.044$ , up to  $\sim 70\%$  of the beam is lost during the 700 ms period, whereas for  $\beta = 0.140$  it only amounts to  $\sim 8\%$ . Hence, suggesting

<sup>3</sup>The purity of the actual distribution of residual gasses in the vacuum chamber is affected by gases introduced by the RGA (Residual Gas Analyzer) filaments during the gas scan measurements. Thus, the high abundance of complex molecular gases obtained (hydro-carbons, eg.  $CH_4$  and  $CO$ ). The high pressure, as opposed to measurements previously reported ( $\sim 2 \times 10^{-11}$ Torr), is likely due to the vacuum problem experienced on 1/17/96 at the C6 superperiod location.

Booster running schemes of higher energies and shorter acceleration cycles (higher  $dB/dt$ 's) in order increase the beam survival time<sup>4</sup>. In addition, one can also observe that at the measured vacuum conditions the beam loss is higher than predicted for all cases except for  $\beta = 0.088$ , where the predicted loss rate is slightly higher, and for  $\beta = 0.102$  where a closer agreement is obtained. For the lowest momentum case ( $\beta = 0.044$ ), analysis shows that either the average ring pressure or the total charge exchange cross section would have to increase by almost a factor of three in order to produce the observed loss rate (refer to Table I.). In general, the overall disagreement suggests that the losses are not solely attributed to beam-gas charge exchange interactions.

It is important to note that we have adopted an additive rule when calculating the capture and stripping cross sections with the residual molecular gas. In other words, we have assumed that at the ion energies involved, the target molecules appear as a collection of individual atoms, whereby the molecular forces can be neglected. Thus, the predicted total cross section is determined by adding together the individual cross sections for each atom in the molecule. Wittkower and Betz [8] have noted that in the treatment of ion-target systems with complex molecular gases, the contributions do not necessarily add in a linear fashion, and as a net result the calculated cross sections are overestimated. Therefore, it is necessary to keep in mind that the theoretical loss rates are likely to be of even smaller magnitude.

The surprising agreement observed for  $\beta$  of 0.088 and 0.102 is not consistent with the findings of previous studies [2]. Even though the data at these energies yielded a poorer least squares fit, it is clear that the measured beam loss more closely approaches the predicted beam-residual gas induced loss. We note that a slight pressure degradation in the Booster vacuum was observed at the C6 injection location a few hours before this measurement was taken. However, the observed effect produced by a small pressure bump would be the opposite under these conditions. The results are summarized graphically in Figure 6, which shows the dispersion between the predicted and measured average loss rates. The overall trend would suggest that at the lower energies ( $\beta < 0.088$ ) studied, some other mechanism other than beam-gas charge exchange is responsible for the losses, and as the beam energy increases the loss rates become comparable to those produced by beam-gas interacting processes.

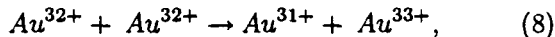
Beam losses were also explored as a function of various intensities. In this case, the Booster input number

<sup>4</sup>Such schemes are however constraint by the Booster main magnet power supplies, the RF systems, and the foil stripping efficiencies in the BTA(Booster to AGS)line for injection into the AGS.

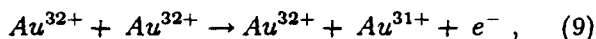
of Gold ions was increased by solely varying the Tandem beam current aperture<sup>5</sup>, and data was acquired at a fixed beam momentum of 82.3/nucleon/c (corresponding to  $\beta = 0.088$ ). It is determined from the various intensity scans, that the average beam loss rate is not constant at a fixed momentum, but rather that it is a monotonically increasing function of the injected number of ions (see Figure 7). In addition, a departure from the predicted beam-gas charge exchange induced loss rate is apparent as the number of ions increases. This result is not expected, since charge exchange (beam-gas) induced losses is not an intensity dependent mechanism. On the other hand, it could be understood in terms of other possible loss processes which might be at work, e.g. intra-beam charge exchange and the possibility of vacuum pressure deterioration due to beam induced gas desorption and/or beam losses throughout the injection part of the cycle. Other intensity dependent processes, such as space charged induced stopbands, and coherent instabilities are not expected to play a role at the ion intensities involved. In the following we quantify the contributions of intra-beam charge exchange reactions as a possible mechanism for beam loss in the Booster. Discussion of the vacuum pressure deterioration will be treated in section 4.

### 3 INTRA-BEAM CHARGE EXCHANGE

There are two relevant reactions by which  $Au^{32+}$  ion-ion charge changing collisions can lead to particle loss in the Booster[3]: electron capture via



with cross section  $\sigma_c(E)$ ; and by ionization through



with cross section  $\sigma_i(E)$ , where  $E$  denotes the relative ion colliding energy. The total beam loss cross section  $\sigma_T(E)$  is then given by

$$\sigma_T(E) = 2(\sigma_c + \sigma_i), \quad (10)$$

since two particles are lost per reaction (8), and both reactants can simultaneously act as projectile and target particle. The total cross section (10) for the combined process (8) and (9) has never been determined experimentally for  $Au^{32+}$ .

<sup>5</sup>Increasing the Tandem aperture correspondingly increases the beam size. Hence, we expect the possible contribution to vacuum degradation resulting from beam losses at the inflector throughout the injection phase-space painting process (Pressure readings were not taken as the aperture was changed. This should be look at closely in future studies).

Following Budicin et al.[9], we use the beam temperature approach in order to extrapolate the rate coefficient and the relative colliding energy of the ions allowing an estimate of the cross section for particle loss. Using this model, the interaction energy of the ions can be determined from the longitudinal momentum spread of the beam and the transverse velocity dispersion arising from the betatron oscillations about the equilibrium orbit. Given the beam and machine parameters during the Booster study which varied beam intensity,  $Au^{32+}$  ions with rest mass  $M_{Au^{32+}} = 1.83457 \times 10^5$  MeV/c<sup>2</sup>, charge state  $Q = +32$ , kinetic energy  $E_{kin} = 0.714$  GeV, relativistic parameters  $\beta = 0.088$  and  $\gamma = 1.0039$ , r.m.s emittances  $\varepsilon_{x(r.m.s)} \sim 73\pi \times 10^{-6}$  m rad, and  $\varepsilon_{y(r.m.s)} \sim 34\pi \times 10^{-6}$ , betatron tunes  $\nu_x = 4.720$  and  $\nu_y = 4.820$ , momentum spread  $\delta p/p \sim 2.0 \times 10^{-3}$ , and the Booster average radius  $\bar{R} = 32.114$  m, we can calculate the interaction energy for each degree of freedom<sup>6</sup>. We then obtain

$$\delta W_{long} = \frac{1}{2} M (\delta v)^2 = \frac{1}{2} M_{Au^{32+}} c^2 \beta^2 \left( \frac{\delta p}{p} \right)^2 = 2.84 \text{ keV}, \quad (11)$$

$$\delta W_{trans_x} = \frac{1}{2} M v_x^2 = \frac{1}{2} E_{kin} \varepsilon_{x(r.m.s)} \frac{\nu_x}{\bar{R}} = 3.83 \text{ keV}, \quad (12)$$

and

$$\delta W_{trans_y} = \frac{1}{2} M v_y^2 = \frac{1}{2} E_{kin} \varepsilon_{y(r.m.s)} \frac{\nu_y}{\bar{R}} = 1.82 \text{ keV}. \quad (13)$$

Thus, since the interacting energies are of comparable magnitude, we approximate the velocity field as nearly isotropic, and hence the beam to be close to an equilibrium state. It follows that we can treat the beam as a gas with an ion average distribution of energies characterized by the beam temperature

$$\frac{3}{2} k_B T_{beam} = \frac{1}{2} M_{Au^{32+}} \left( \sqrt{(\delta v)_{long}^2 + (v)_{trans_x}^2 + (v)_{trans_y}^2} \right)^2 = 8.49 \text{ keV}, \quad (14)$$

where  $k_B$  is the Boltzmann constant.

<sup>6</sup>The r.m.s emittance was not measured during the study. However, we estimate its value in the Booster from a beam size measurement taken on the first multiwire (MW006) in the BTA line[10], while extracting  $Au^{32+}$  ions at  $E_{kin} = 95.23$  MeV/n within a few hours after the study was undertaken ( $N \sim 1.7 \times 10^9$  ions). The change in beam size due to intensity increase is not taken into account.



### 3.1 MODELING INTRA-BEAM CHARGE EXCHANGE AND TOTAL BEAM LOSS

In the comoving frame of the particles in the beam, the number of Au<sup>32+</sup> ions decreases according to the relation

$$\frac{dN}{dt} = -R(t), \quad (15)$$

where  $R(t)$  denotes to the reaction rate, and it depends on the beam density, cross section, energy and beam volume[9] by

$$R(t) = \frac{1}{2} \int_V n^2(r, t) \langle \sigma_T v \rangle dV. \quad (16)$$

Here,  $\langle \sigma_T v \rangle$  represents the rate coefficient for particle loss,

$$\langle \sigma_T v \rangle = \int_0^{E_{\max}} \sigma_T(E) v f(E) dE, \quad (17)$$

and  $\sigma_T(E)$  is the total cross section as described in eq.(10),  $E$  the relative colliding energy,  $v$  the relative velocity in the ion-ion collisions, and  $f(E)$  the distribution of energies which we assume to follow the Maxwell-Boltzmann distribution function.

In order to indirectly estimate the total cross section  $\sigma_T$ , we assume the mean square fluctuations of the ions is small, that is;  $(\frac{\langle v^2 \rangle - \langle v \rangle^2}{\langle v \rangle^2} \ll 1)$ , and approximate the rate coefficient as  $\langle \sigma_T v \rangle \simeq \langle \sigma_T \rangle \langle v \rangle$ . Where  $\langle v \rangle = \sqrt{8kT_{beam}/M_{Au^{32+}}}$  is the mean relative ion velocity possessed by the Maxwellian distribution of ions in the beam. Thus, if this condition is satisfied, the rate coefficient will be a quantity averaged over the velocity field, and the estimate for the total cross section will only be meaningful at the mean relative velocity of the distribution.

Further, the debunched beam is assumed to have a uniform density and constant volume throughout the machine lattice<sup>7</sup>; that is,

$$n(r, t) = n(t) = \frac{N(t)}{V}, \quad (18)$$

where  $N(t)$  is the number of ions in the ring as a function of time and  $V_{beam}$  the beam volume given by

$$V_{beam} \simeq 4\sqrt{\beta_x \varepsilon_x(r.m.s)} \sqrt{\beta_y \varepsilon_y(r.m.s)} l_{beam}. \quad (19)$$

Here,  $\overline{\beta_{x,y}}$  are the average horizontal and vertical Booster lattice beta functions (by definition,  $\overline{\beta_{x,y}} = \bar{R} / \nu_{x,y}$ ),

<sup>7</sup>The problem can be treated more rigorously by taking into account variation in beam density due to strong focusing. In such case, the volume has dependence  $\beta_H(t)$  and  $\beta_V(t)$  for different lattice elements as a function of time[9], with more interactions occurring where  $\beta_{x,y \min}$ , and the ion density is higher.

and  $l_{beam}$  the beam length (the Booster circumference,  $C = 201.78$  m). We then acquire for the reaction rate

$$R(t) = \frac{1}{2} \frac{N^2(t)}{V} \langle \sigma_T v \rangle. \quad (20)$$

By substitution into eq.(15), the rate of beam loss in the Booster due to ion-ion charge exchange interactions can be expressed as

$$\frac{dN}{dt} = \frac{\langle \sigma_T v \rangle}{2V} N^2(t). \quad (21)$$

The solution for eq. (21) reads

$$N(t) = \frac{1}{\frac{1}{N_0} + \kappa t}, \quad (22)$$

where again  $N_0 = N(t = t_{RFoff})$  denotes the number of ions in the Booster at RF turn off time, and  $\kappa = \frac{\langle \sigma_T v \rangle}{2V}$ , the rate constant ( $s^{-1}$ ).

Since the ion loss due to beam-gas charge exchange interactions cannot be neglected, a more satisfactory description of the total beam loss requires that we sum the contributions from eq.(7) and eq. (21), yielding the model equation [11]

$$\frac{dN}{dt} = -\alpha N(t) - \kappa N^2(t). \quad (23)$$

Once again,  $\alpha$  refers to the average loss rate due to beam-gas interactions (eq.(7)), and  $\kappa$  the intra-beam charge exchange rate constant. The above differential equation can be solved by separation of variables yielding the expression

$$N(t) = \frac{\alpha}{\alpha(\frac{1}{N_0} + \frac{\kappa}{\alpha}) \exp(\alpha t) - \kappa}. \quad (24)$$

Note that for  $\kappa = 0$  we recover eq. (7).

### 3.2 RESULTS

To test the validity of model equation (22) and (24) and determine the average loss rate  $\alpha$ , rate constants  $\kappa$  and coefficients of particle loss  $\langle \sigma_T v \rangle$ , we performed a nonlinear least square fit, (using Levenberg-Marquardt's method) to the various ion intensities data scans taken. For purposes of comparison, the predicted and best fit to equation (7) representing solely beam-gas charge exchange are also presented. Figures 8-13 display the evolution of the beam intensity along with the best fitted equations. For Figure 8 and 9, only  $\sim 200$  data points were sampled, whereas for the remainder of the intensity traces, sets on the order of 1600 points were taken. Table II presents the results obtained for the fitted parameters. The standard deviations were extracted from the variation obtained from each subsequent fit to the

data. Thus, the rate constants obtained represent average values.

As can be seen from Table II, the average rate constants obtained indicates that as an upper limit,  $\sim 2$  out of  $10^9$   $\text{Au}^{32+}$  ions are lost per second, making the contributions of intra-beam charge exchange in the Booster absolutely negligible. Secondly, we note the anomalously high rate coefficients obtained. In comparison, Muller et al. [12] measures dielectronic recombination rate coefficients of  $10^{-7}\text{cm}^3\text{s}^{-1}$  for  $\text{Au}^{25+}$ . In our calculation, only uncertainties in the beam volume  $V_{\text{beam}}(\sim 2.73 \times 10^5\text{cm}^3)$  would affect this result, and we regard our estimates as a reasonable upper limit. However, it is important to keep in mind that in the current analysis we are assuming that the beam losses are attributable to only charge exchange processes. In the presence of other possible (unknown) beam loss mechanisms, the magnitude of the fitted rate constants as described by eq.'s (22) and (24) are subjected to inaccuracies.

The estimated total cross section is consequently also of high magnitude. Since these measurements represent the first cross sectional estimates for  $\text{Au}^{32+}\text{-Au}^{32+}$  collisions, we are unable to make absolute judgements. Nevertheless, we compare the experimental results of Melchert et al.[3] with  $\text{Au}^{-1}$  negative ions, which yielded  $\sigma_T \sim 3 \times 10^{-15}\text{cm}^2$ . We emphasize that these relative differences may be due to the limited data, validity in the model, and/or the different electronic structure for the respective ion species.

An essential feature providing clues about the validity of the model equations and the results outlined above, is the obtained dispersion for the rate constants from each intensity scan. If the model equations are to be regarded as satisfactory descriptors of the beam losses observed, we require the fitted rate parameters to be constant, independent of the beam intensity. As we can observe, the dispersion for  $\kappa$  in eq. (24) at the  $2\sigma$  level of confidence is larger in magnitude than the yielded average value, putting into question its validity<sup>8</sup>. Moreover, the best fitted beam-gas average loss rate  $\alpha$  for eq. (24) is  $0.58 \pm 0.49 \text{ s}^{-1}$ , which yields the total cross section  $\sigma_t = (1.01 \pm 0.86) \times 10^{-16}\text{cm}^2$ . Thus, in rough agreement with the cross section presented in Table I for the corresponding energy ( $2.98 \times 10^{-17}\text{cm}^2$ )<sup>9</sup>. In contrast, the fitted rate constant  $\kappa$  in eq. (22) displays minimum dispersion, and interestingly, it differs to that of eq.(24) by roughly an order of magnitude. With these notable

<sup>8</sup>A more definite quantitative confidence analysis for these results would require a larger data sample. Although, the construction of synthetic data sets through the use of Monte Carlo simulation methods is equally suitable.

<sup>9</sup>However, caution must be taken since the result for  $\sigma_T$  ( $\beta = 0.088$ ) in Table I is likely to also have a large associated uncertainty.

features in mind, we regard the intra-beam constants and cross sections extrapolated from eq. (22) as merely estimates.

## 4 BOOSTER VACUUM DETERIORATION

The increase in beam loss with the number of ions suggests the beam is affecting the residual molecular gas in the Booster vacuum chamber. Indeed, a "multiple pulse memory effect" has been observed in previous studies, where allowing the machine to cool ( $\sim 1$  min) substantially improves the loss rate for the next few subsequent cycles [1]<sup>10</sup>.

Table III. displays the calculated ring pressure increase  $\frac{P_{\text{Fit}}}{P_{\text{Measured}}}$  necessary in order to reproduce the ideal fit to eq. (7). Assuming the cross sections have not been underestimated, we speculate this pressure deterioration can be attributed to outgassing produced from beam losses resulting presumably throughout the injection process (e.g. at inflector), and to possible desorption processes[1].

To explore the discrepancy obtained between the calculated and measured beam loss rates, we consider how the ring average pressure changes with the injected number of  $\text{Au}^{32+}$  ions. A relationship between the decay time constant  $\tau$  (inverse beam loss rate) and the ring pressure can be phenomenologically established by introducing a quadratic factor in time in model equation (7), which we rewrite as

$$N(t) = N_0 \exp\left[-\frac{t}{\tau} - \left(\frac{t}{\tau}\right)^2\right]. \quad (25)$$

Where the parameter  $\frac{1}{\tau}$  corresponds to the average loss rate  $\alpha$  (eq. (6)). Writing eq. (6) in terms of the average ring pressure ( $P = nk_B T$ ) and differentiating with respect to  $\tau$  yields

$$-\frac{1}{\tau^2} = \frac{dP}{d\tau} \cdot \frac{\sigma_T \beta c}{k_B T}. \quad (26)$$

Substituting into eq.(25) then gives

$$N(t) = N_0 \exp\left[-\left(\frac{P\sigma_t\beta c}{k_B T}\right)t + \left(\frac{dP}{d\tau} \frac{\sigma_T\beta c}{k_B T}\right)t^2\right]. \quad (27)$$

Thus, for a given beam energy, number of  $\text{Au}^{32+}$  ions in the ring, and vacuum conditions (P,T) we can study the

<sup>10</sup>In addition, since the study was performed on Booster USER2 while USER1 was active, this multiple pulse memory effect can consequently affect the vacuum conditions when the USER2 (due to USER1) beam loss data was taken. Thus, yielding a larger disagreement between model and theory.

evolution of the ring pressure as a function of the decay time constant.

We have fitted eq. (27) to the beam loss data gathered at the various intensities ( $\sim 4 \times 10^8 \rightarrow \sim 1.2 \times 10^9$  ions). Fig. 14 and 15 presents the obtained average loss rate  $\alpha$  and  $\frac{dP}{dt}$  (Torr/sec) respectively for the intensities explored. We expect  $\frac{dP}{dt}$  to increase and saturate as the decay time constant decreases (number of ions increases). However, the results show there is no clear apparent trend between the two quantities. Interestingly however, the positive magnitude for the  $\frac{dP}{dt}$  extrapolated indicates the ring pressure is actually improving as the beam circulates the ring. This result could be attributed to considerable vacuum pressure degradation at injection and acceleration. Thus, assuming the beam induced pressure deterioration is negligible after RF turn-off, the number density of outgassing particles will decrease as the cycle evolves, and the vacuum pumps remove the released gas at the limiting pumping speed (gas composition dependent). This vacuum performance ( $\frac{dP}{dt} \sim 6 \times 10^{-11}$  Torr/sec at max.) is expected from the titanium sublimation and ion pumps throughout the Booster ring<sup>11</sup>. Nevertheless, considering the small data sample available and the scatter obtained, these results are by no means conclusive. It is suggested that a larger range of intensities is explored in future studies, and furthermore, that pressure readings be monitored closely as the Tandem beam current aperture is changed in order to verify any correlations with these results and further test the validity of model eq. (27).

It is also of interest to investigate the long term time dependence of the beam average loss rate by constructing an hypothetical four second length magnetic flat top. Assuming the state of the machine remains unchanged, the goal of such experiment is to test the departure from a perfect exponential and study the loss rate behavior (eq. (7)) over longer time scales. Fig. 16 depicts such curve constructed from the set of current transformer traces taken at a  $\beta = 0.088$ . It is observed that a simple exponential (eq. (7)) does not produce the proper functionality (steepness at high intensities) in order to globally fit the curve. For comparison, a fit to the initial current transformer trace used in the Global fit (that of Fig.8 with  $N_0 \sim 1.2 \times 10^9$  ions) yielded an average loss rate  $\alpha = 0.511s^{-1}$ . Whereas, the Global fit to the exponential yields an average loss rate roughly a factor of two smaller ( $\alpha = 0.28s^{-1}$ ) for the same initial number of ions at RF turn off (but longer flat-top). Alternatively, the quadratic dependence in eq.'s (23) and (27) reproduce more closely the behavior of the data. Where for

<sup>11</sup>Booster vacuum data collected during an observed vacuum deterioration at the C6 location shows the rate of pressure improvement is in agreement with the numbers obtained above.

eq. (27),  $\alpha = 0.511s^{-1}$ , with equal magnitude to the fit to eq. (7) (600 ms flat-top). We keep in mind that these intrinsic differences can be attributed to different machine histories associated with each individual current transformer trace. Configuration of a similar machine set-up should be considered in future studies.

## 5 CONCLUSION

To conclude, we find that in the consideration of charge exchange processes only beam-gas charge exchange can appreciably contribute to beam losses in the Booster (at max.  $\sim 30\%$  for the vacuum conditions stated). The average loss rates obtained reflect that the percentage of beam losses is a sensitive function of the beam energy. With the loss significantly minimized as the beam energy increases ( $\beta = 0.044 \rightarrow \beta = 0.140$  :  $\sim 70\% \rightarrow \sim 8\%$ ). In addition, we noted the large variation obtained between the predicted and measured beam loss rates at the lower beam energies studied, which hints at the presence of some other mechanism at work. At this stage, we are unable to explain the observed difference fully; it can only be further explored with the advent of additional data. Also, the observed dependence of beam loss with intensity motivated the inclusion of intra-beam charge exchange and vacuum degradation as a possible loss mechanism. However, the estimated intra-beam rate constant ( $\sim 10^{-9} - 10^{-10}s^{-1}$ ) obtained rules out any contribution from this process in the Booster. Lastly, even though vacuum degradation in the Booster ring could explain some of the results observed for Au<sup>32+</sup> loss, there is no ring pressure variation data available that can be used for confirmation. Hopefully, the studies to be performed during the 1996 Heavy ion run will help resolve some of these problems.

We thank M. Blaskiewicz, T. Roser, H. Hseuh, K. Zeno, C. Gardner, M. Mapes and S. Gill for many stimulating and helpful discussions. Also, we appreciate the essential contribution from the Tandem and AGS accelerator staff for making the studies possible.

## REFERENCES

- [1] M. Blaskiewicz, L.A. Ahrens, H.C. Hseuh, T. Roser, and K. Zeno, "Observation of Intensity Dependent Losses in Au<sup>15+</sup> Beams", 1995 Particle Accelerator Conf..
- [2] T. Roser, L.A. Ahrens, and H.C. Hseuh, "Charge Exchange Studies with Gold Ions at the Brookhaven Booster and AGS", Fourth European Particle Accelerator Conf., pp. 2441-2443.
- [3] F. Melchert, E. Salzborn, I. Hofmann, R.W. Muller, V.P. Shelvelko, Nuclear Instruments and

Methods in Physics Research, A278 (1989) 65-67.

- [4] H.C. Hseuh, Booster Beam Loss Due to Beam-Residual Gas Charge Exchange, Booster Technical Note No.116, BNL, April 20, 1988.
- [5] A.S. Schlachter, J.W. Stearns, W.G. Graham, K. H. Berkner, R.V. Pyle, and J.A. Tanis, Phys. Rev. A27, (1983) 3372.
- [6] H.D. Betz, Rev. Mod. Phys. 44, (1972) 465.
- [7] Discussions with H.C. Hseuh and M. Mapes.
- [8] A.B. Wittkower and H.D. Betz, J. Phys. B, 4, (1971) 1173.
- [9] D. Budicin, I. Hofmann, M. Conte, R. Schulze, F. Melchert, and E. Salzborn, Il Nuovo Cimento, Vol. 106A, N.11, (1993) 1621.
- [10] J. Ryan, Morning Numbers, January 21, 1996.
- [11] Discussions with T. Roser.
- [12] A. Muller et al., Radiative and Dielectronic Recombination, in: Proc. Symp. Cooler Rings (Toyko, 1990), eds. T. Katayama and A. Noda (World Scientific, London, 1991) p.248.

Table I. Comparison between the predicted and measured charge exchange cross sections and average loss rates as a function of different beam momenta. The required average ring pressure increase (or total charge exchange loss rate) in order to reproduce the results is also included as  $\frac{P_{Fit}}{P_{Measured}}$  ( $P_{Measured} = 5.6 \times 10^{-11} Torr$ ).

Table I. Theory vs. Experiment (Au <sup>32+</sup> Beam-Gas Charge Exchange)								
pc (MeV/n)	$\beta$	$\sigma_c [cm^2]$	Predicted $\sigma_s [cm^2]$	Predicted $\sigma_t [cm^2]$	Predicted $\alpha_t [s^{-1}]$	Measured $\sigma_t [cm^2]$	Measured $\alpha_t [s^{-1}]$	$\frac{P_{Fit}}{P_{Measured}}$
41.0	0.044	$1.19 \times 10^{-16}$	$1.72 \times 10^{-17}$	$1.36 \times 10^{-16}$	0.388	$3.69 \times 10^{-16}$	1.049	2.70
54.1	0.058	$8.57 \times 10^{-17}$	$1.30 \times 10^{-17}$	$9.88 \times 10^{-17}$	0.370	$1.69 \times 10^{-16}$	0.635	1.71
82.3	0.088	$3.02 \times 10^{-17}$	$8.59 \times 10^{-18}$	$3.88 \times 10^{-17}$	0.220	$2.98 \times 10^{-17}$	0.159	0.72
95.5	0.102	$1.47 \times 10^{-17}$	$7.41 \times 10^{-18}$	$2.21 \times 10^{-17}$	0.146	$2.19 \times 10^{-17}$	0.144	0.99
131.7	0.140	$1.32 \times 10^{-18}$	$5.40 \times 10^{-18}$	$6.72 \times 10^{-18}$	0.061	$9.89 \times 10^{-18}$	0.089	1.47

Table II. Au<sup>32+</sup> intra-beam charge exchange rate constants and cross sections extrapolated from the nonlinear fits to eq.'s (22) and (24).

Table II. Extrapolated Rate Constants and Cross Sections			
Model Equation	$\bar{\kappa} [10^{-9} s^{-1}]$	$\langle \sigma_T v \rangle [10^{-4} cm^3 s^{-1}]$	$\langle \sigma_T \rangle [10^{-11} cm^2]$
Eq.(22)	$0.38 \pm 0.06$	$2.06 \pm 0.32$	$1.38 \pm 0.22$
Eq.(24)	$1.39 \pm 0.93$	$7.61 \pm 5.11$	$5.12 \pm 3.44$

Table III. Beam-gas charge exchange average loss rate  $\alpha_t$  as a function of  $\text{Au}^{32+}$  intensity. The required pressure increase to agree with the predictions is also presented.

Table III. Average Loss Rate vs. Intensity		
$N_{\text{ORFoff}}(\times 10^8 \text{ions})$	$\alpha_t [s^{-1}]$	$\frac{P_{\text{fit}}}{P_{\text{measured}}}$
4.39	0.161	0.732
6.31	0.218	0.988
7.98	0.248	1.125
8.28	0.251	1.138
10.76	0.304	1.378
12.47	0.511	2.316

## Figure Captions

**Figures 1-5.** Booster beam loss observed as a function of momenta ( $\beta$ ). The solid line represents a least squares fit to the data. The dashed lines correspond to the predicted electron capture, stripping loss rates and the net contribution due to beam-gas charge exchange (eq.(7))

**Figure 6.** Comparison between the predicted and measured average loss rates for the various beam momenta studied. The solid line refer to the measured average loss rates  $\alpha_t$  in eq.(7). The dashed lines are the calculated capture ( $\alpha_c$ ) and stripping ( $\alpha_s$ ) loss rates along with their summed contribution ( $\alpha_t$ ).

**Figure 7.** Average loss rates obtained as a function of  $\text{Au}^{32+}$  intensity for  $\beta = 0.088$ . Note the monotonic increase in the loss rate with  $\text{Au}^{32+}$  intensity.

**Figures 8-13.** Beam loss observed as the  $\text{Au}^{32+}$  intensity is varied. The data is fitted to the beam-gas charge exchange eq.(7), the intra-beam contribution described by eq.(22), and the total beam loss model equation (24). For comparison, the predicted charge exchange beam loss is also included. Note how the prediction approaches the measured loss rate as the input number of  $\text{Au}^{32+}$  is decreased.

**Figure 14.** Average loss rate extrapolated from fit to eq.(27).

**Figure 15.** Pressure variations as a function of the decay time constant for the various intensities studied.

**Figure 16.** Hypothetical four second flat-top constructed from the current transformer data taken at  $\beta = 0.088$ . Data was not taken for  $\text{Au}^{32+}$  intensities in the range  $4.0-5.5 \times 10^8$  ions. Note the unsatisfactory fit to an exponential eq.(7).

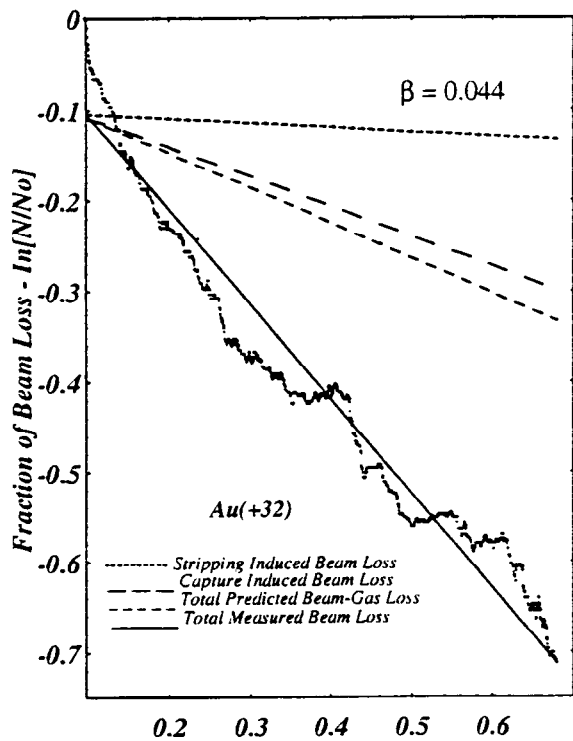


Figure 1

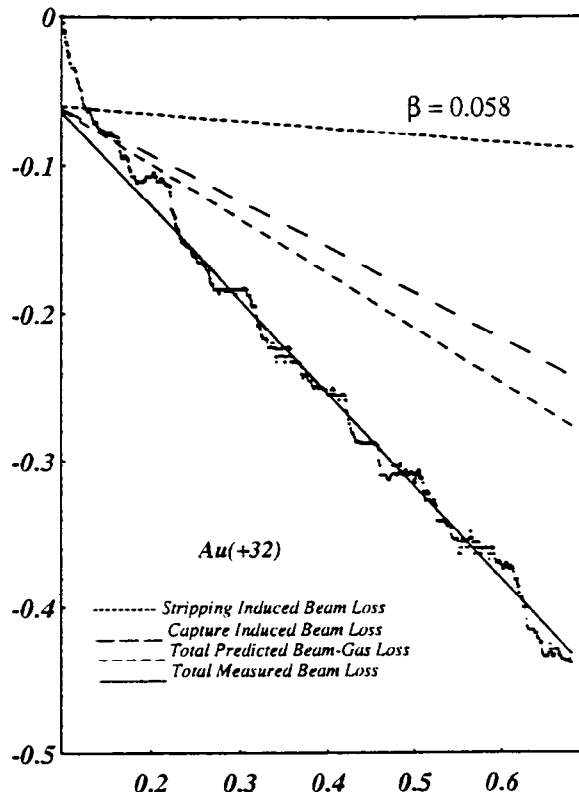


Figure 2

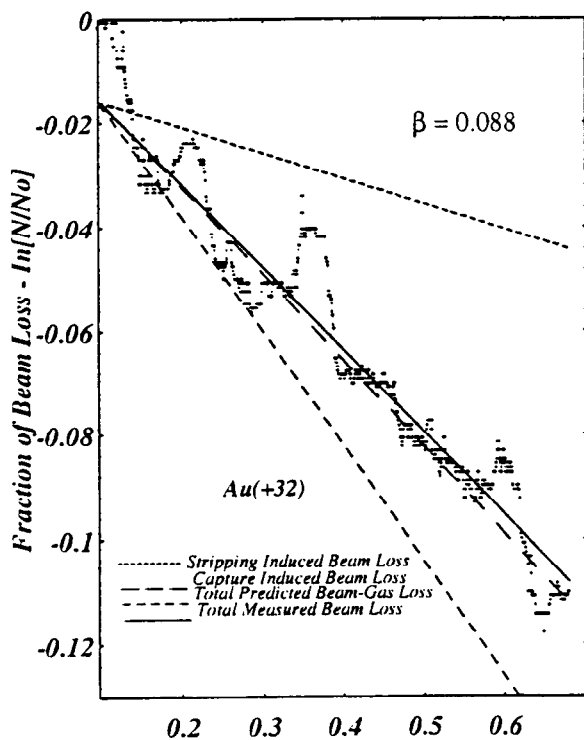


Figure 3

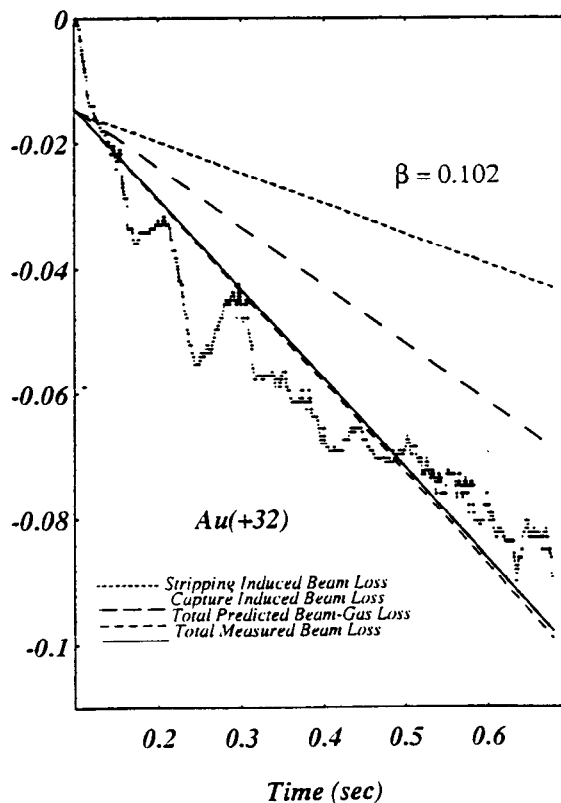


Figure 4



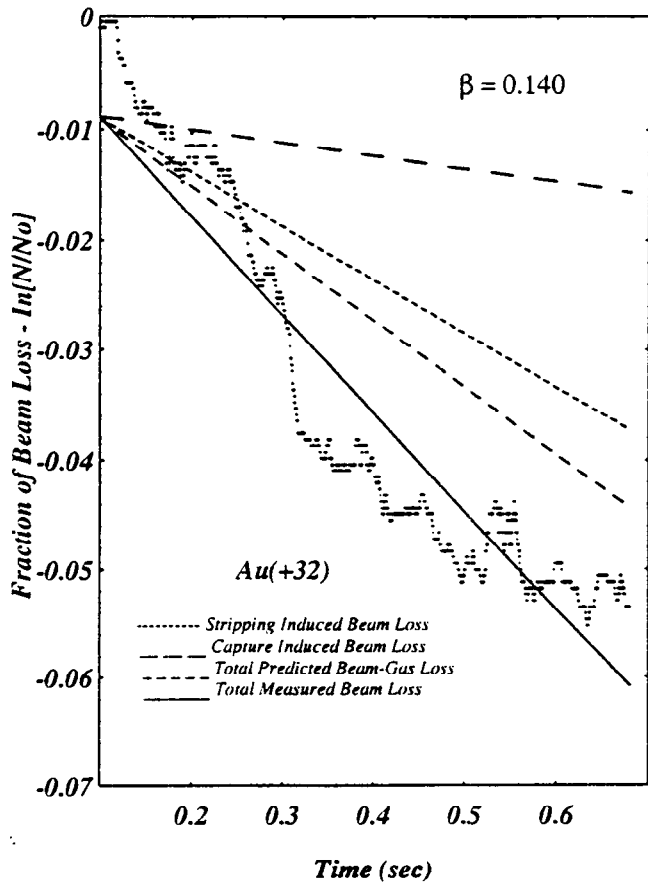


Figure 5

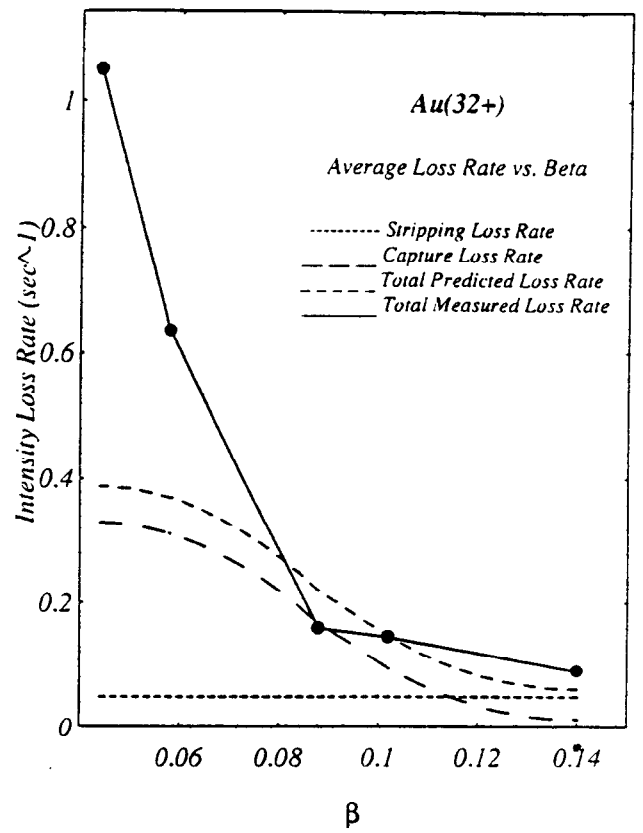


Figure 6

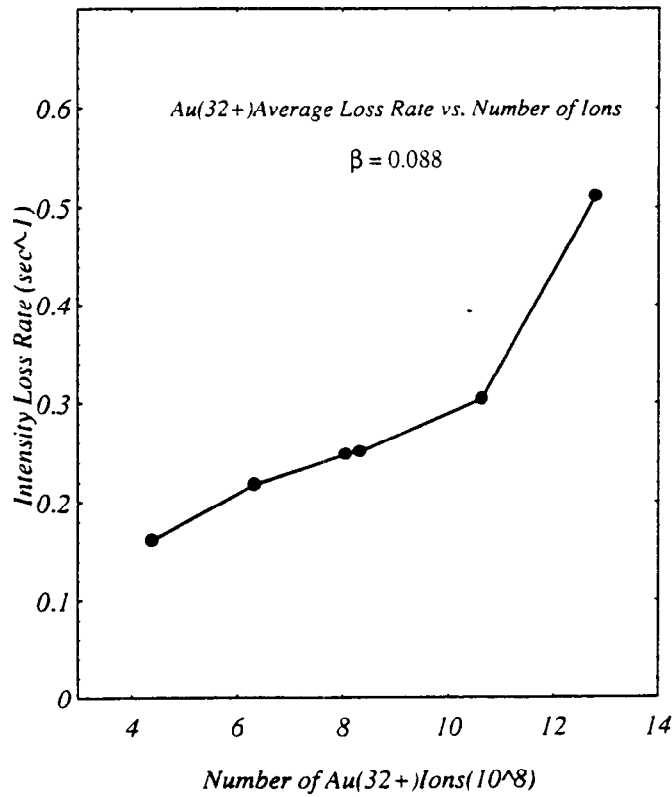


Figure 7

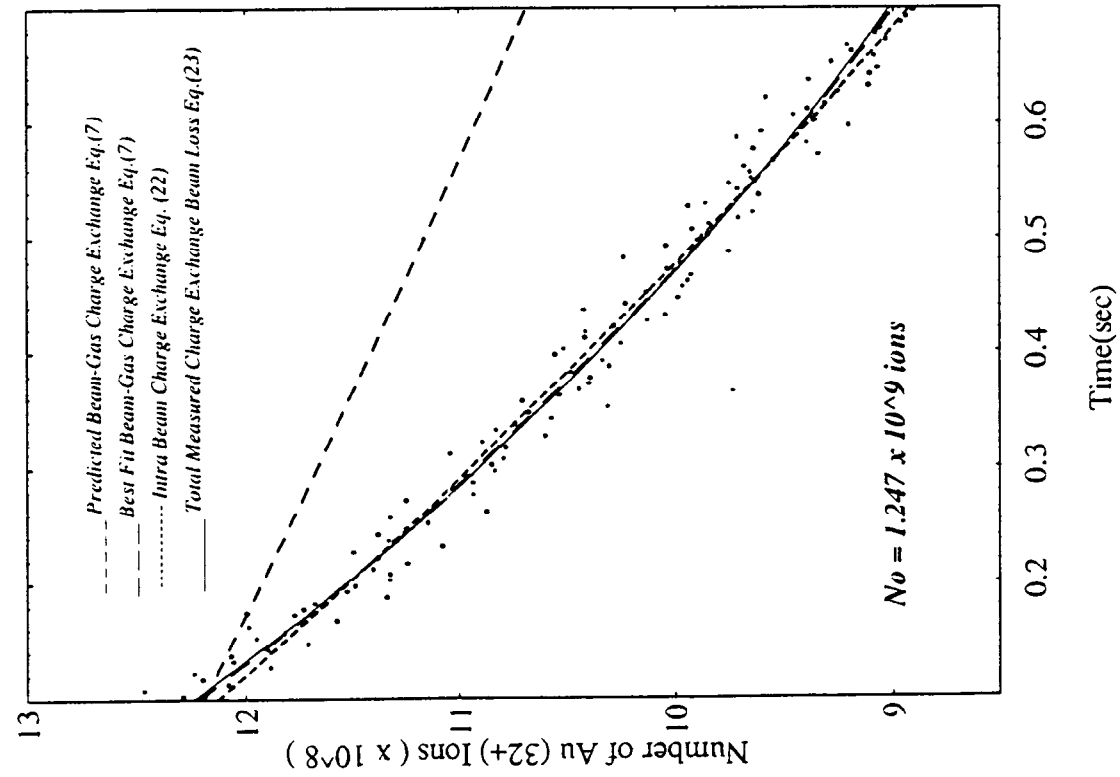


Figure 8

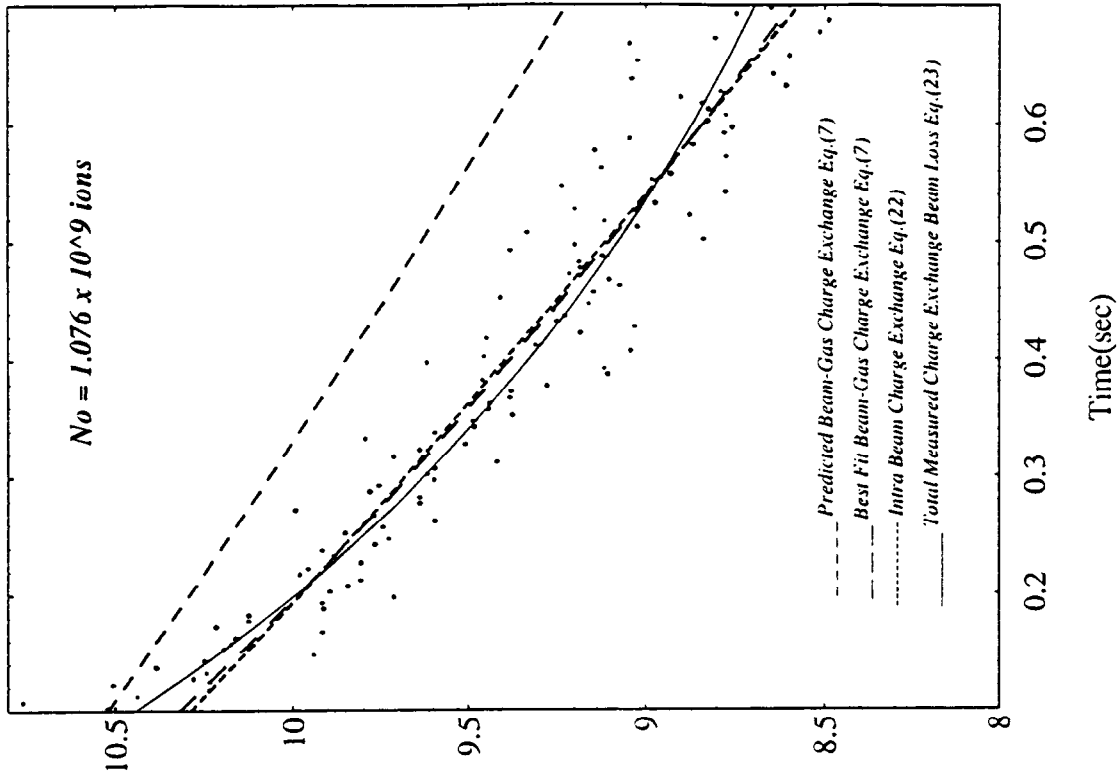


Figure 9

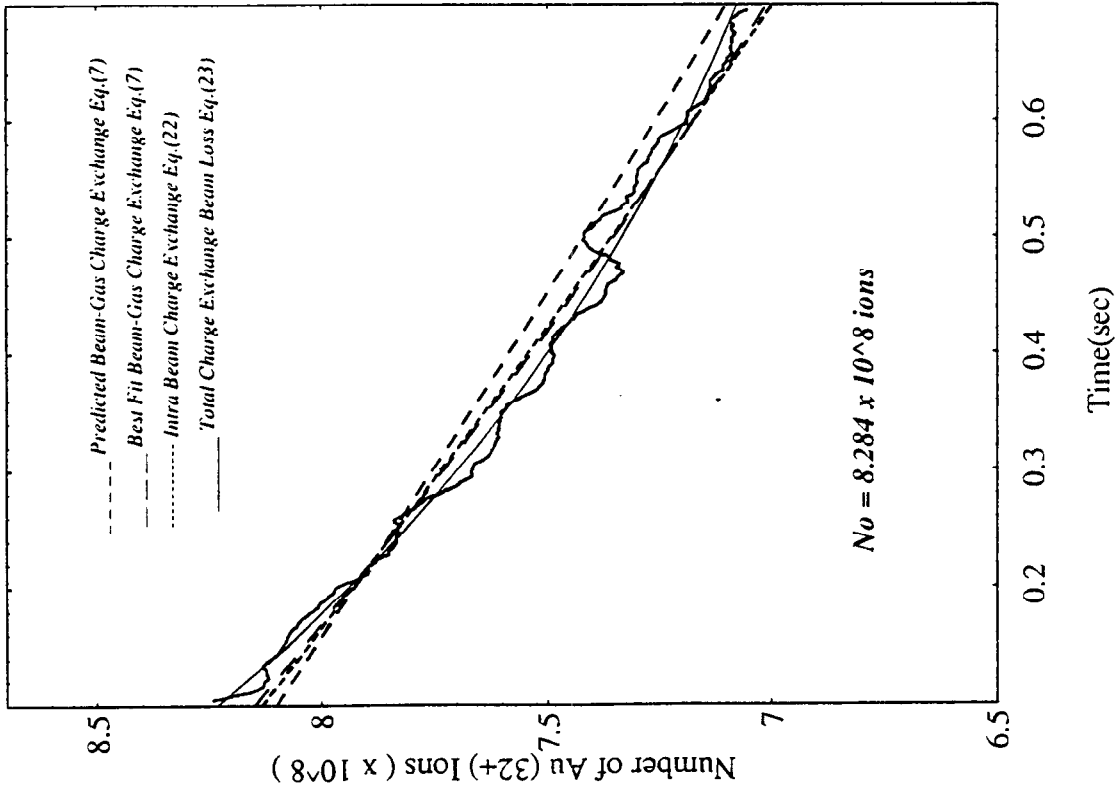


Figure 10

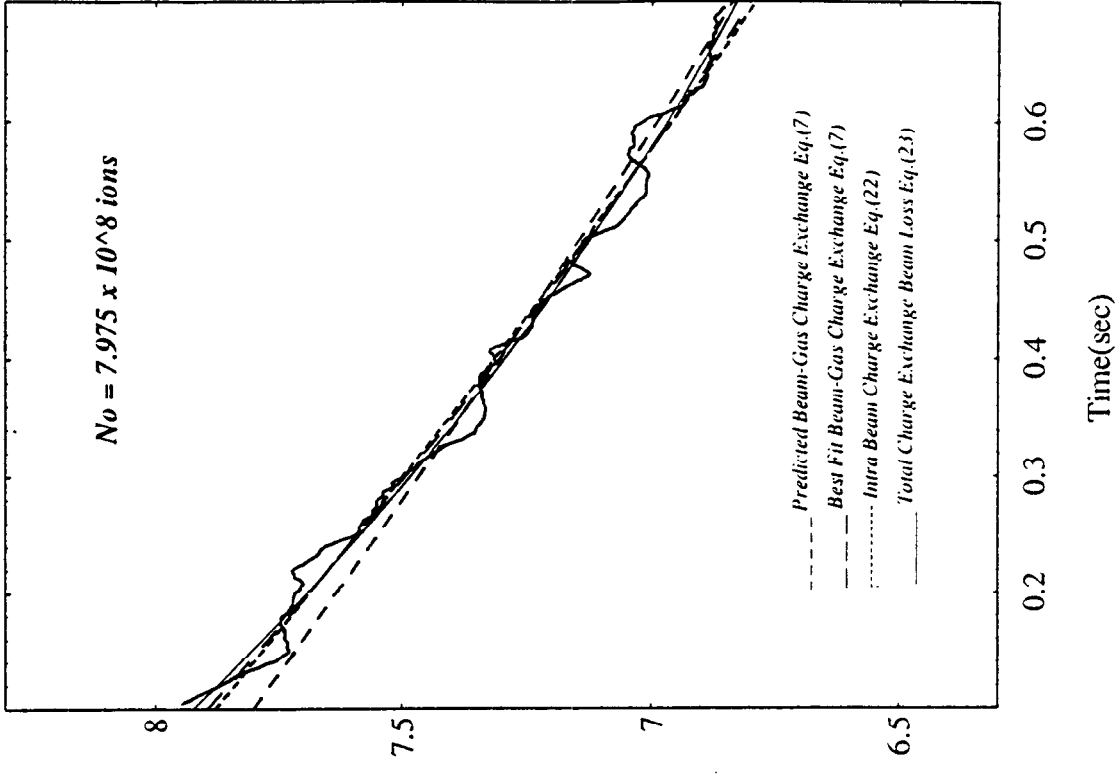


Figure 11

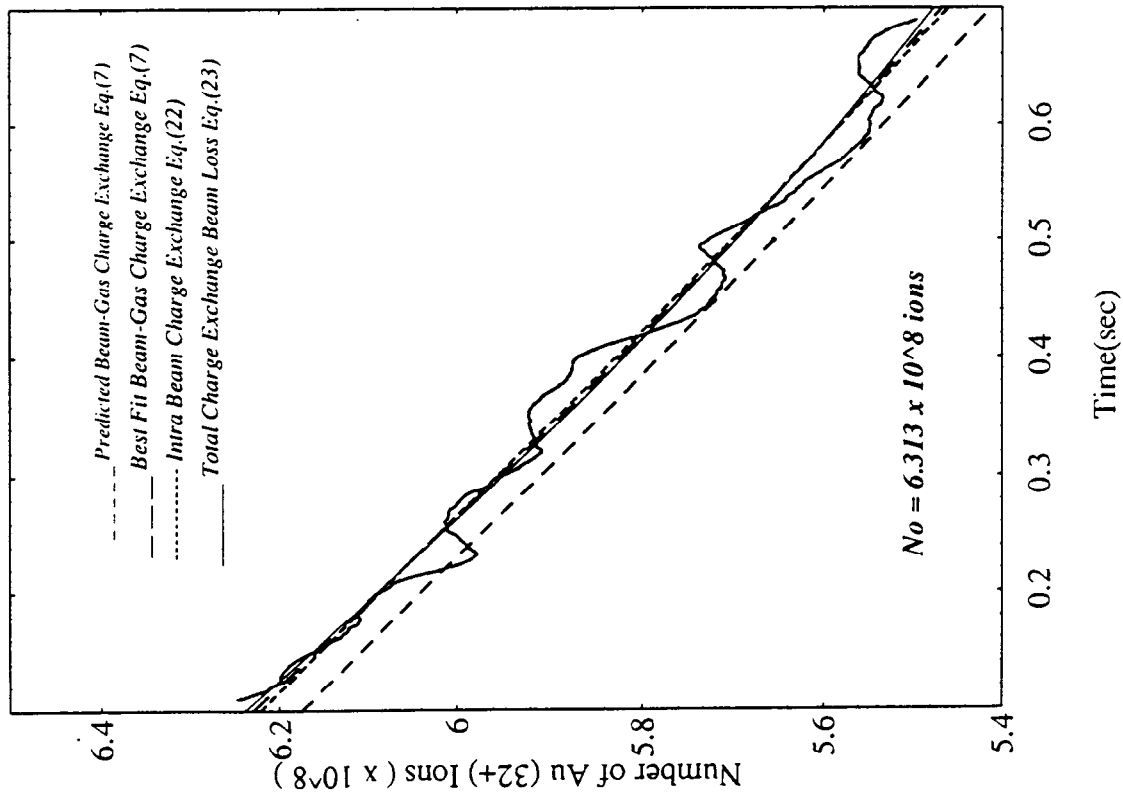


Figure 12

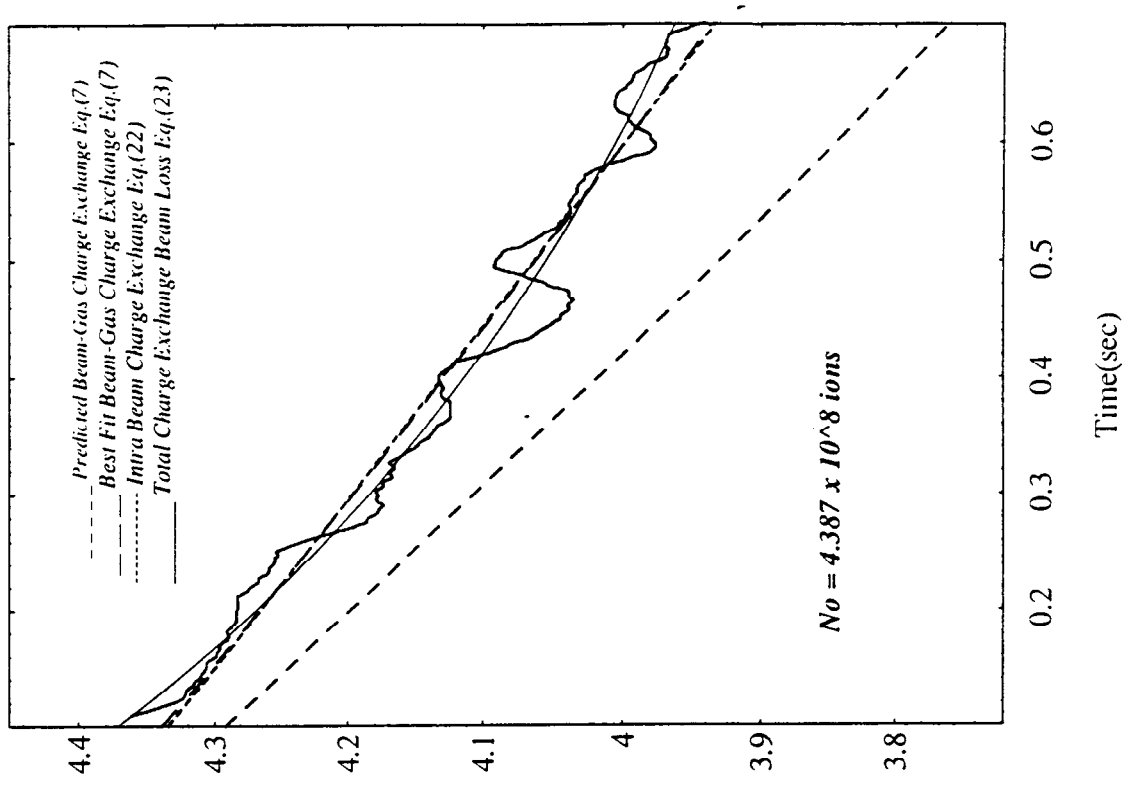


Figure 13

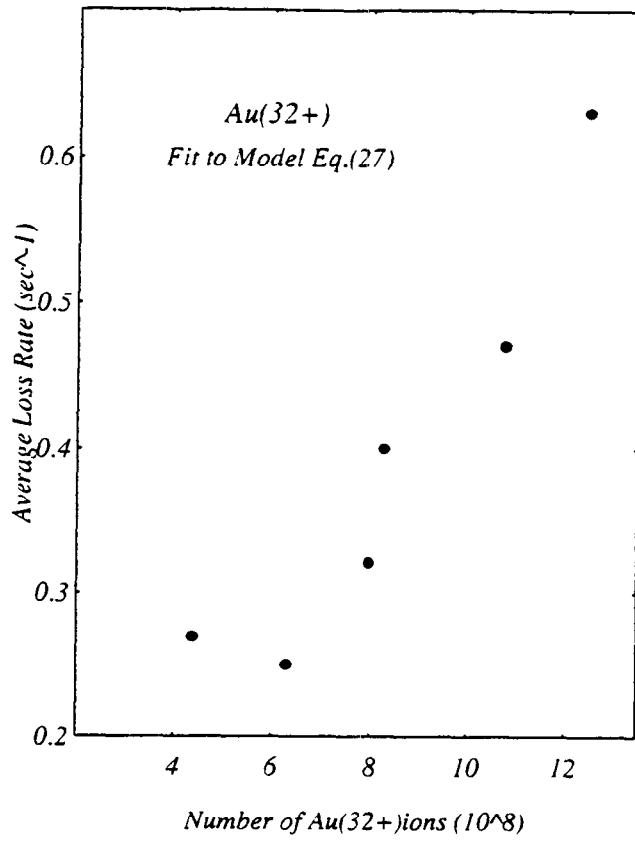


Figure 14

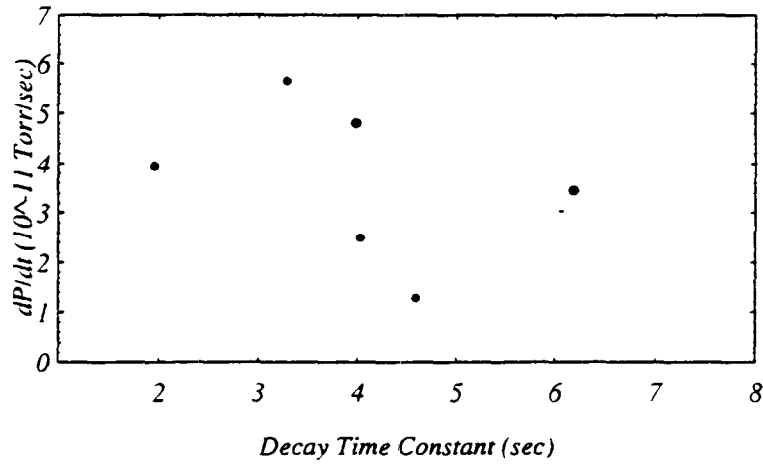


Figure 15

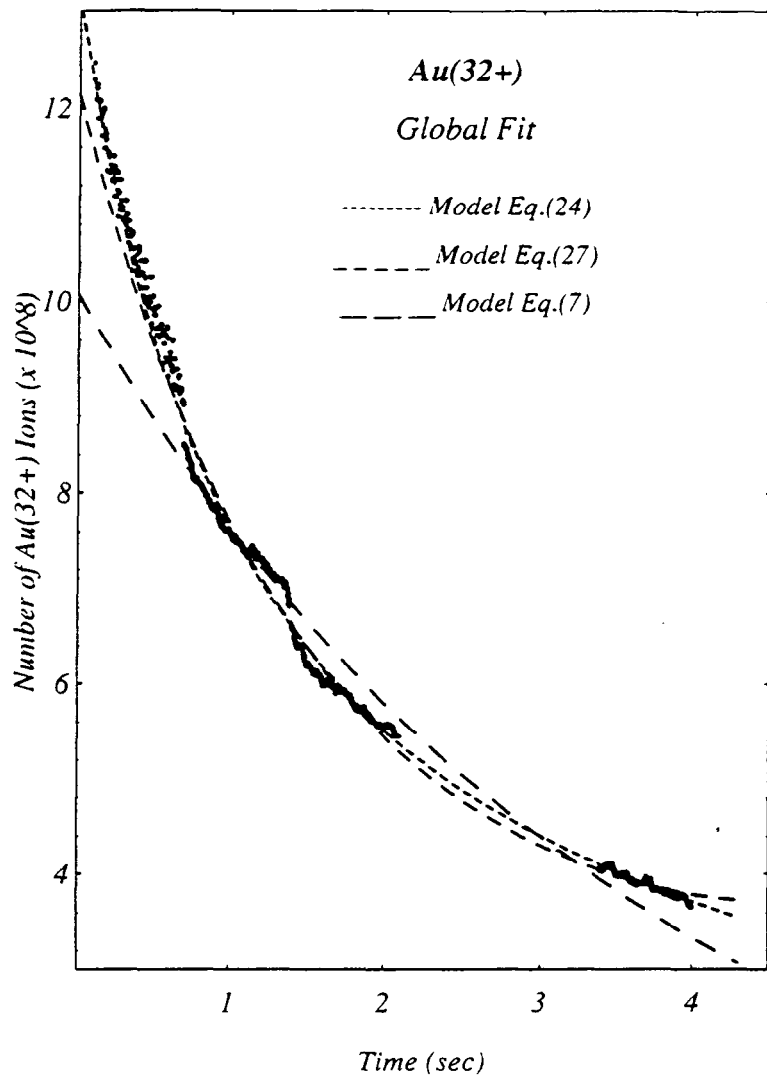


Figure 16